OIKOS

Research

Stability of rocky intertidal communities, in response to species removal, varies across spatial scales

Nelson Valdivia, Daniela N. López, Eliseo Fica-Rojas, Alexis M. Catalán, Moisés A. Aguilera, Marjorie Araya, Claudia Betancourtt, Katherine Burgos-Andrade, Thais Carvajal-Baldeon, Valentina Escares, Simon Gartenstein, Mariana Grossmann, Bárbara Gutiérrez, Jonne Kotta, Diego F. Morales-Torres, Bárbara Riedemann-Saldivia, Sara M. Rodríguez, Catalina Velasco-Charpentier, Vicente I. Villalobos and Bernardo R. Broitman

N. Valdivia (https://orcid.org/0000-0002-5394-2072) ✉ (nelson.valdivia@uach.c), K. Burgos-Andrade, T. Carvajal-Baldeon, V. Escares, B. Gutiérrez, D. F. Morales-Torres, B. Riedemann-Saldivia, S. M. Rodríguez (https://orcid.org/0000-0002-1855-4170), V. I. Villalobos, A. M. Catalán, C. Betancourtt and and S. Gartenstein, Inst. de Ciencias Marinas y Limnológicas, Facultad de Ciencias, Univ. Austral de Chile, Campus Isla Teja, Valdivia, Chile. NV also at: Centro FONDAP de Investigación de Dinámicas de Ecosistemas Marinos de Altas Latitudes (IDEAL), Santiago, Chile. AMC, CB and SG also at: Programa de Doctorado en Biología Marina, Facultad de Ciencias, Univ. Austral de Chile, Valdivia, Chile. – D. N. López (https://orcid.org/0000-0003-2028-8438), E. Fica-Rojas and M. Grossman, Inst. de Ciencias Ambientales y Evolutivas, Univ. Austral de Chile, Valdivia, Chile. DNL also at: Center of Applied Ecology and Sustainability (CAPES), Pontificia Univ. Católica de Chile, Santiago, Chile. EF and M G also at: Programa de Doctorado en Ciencias mención Ecología y Evolución, Facultad de Ciencias, Univ. Austral de Chile, Valdivia, Chile. – M. Araya, Centro FONDAP de Investigación de Dinámicas de Ecosistemas Marinos de Altas Latitudes (IDEAL), Santiago, Chile. – M. A. Aguilera (https://orcid.org/0000-0002-3517-6255), Depto de Ciencias, Facultad de Artes Liberales, Univ. Adolfo Ibáñez, Diagonal Las Torres, Santiago, Chile. – J. Kotta (https://orcid.org/0000-0002-4970-6755), Estonian Marine Inst., Univ. of Tartu, Tallinn, Estonia. – C. Velasco-Charpentier (https://orcid.org/0000-0003-4285-3565), Centro de investigación Gaia Antártica, Univ. de Magallanes, Punta Arenas, Chile. – B. R. Broitman (http://orcid.org/0000-0001-6582-3188), Depto de Ciencias, Facultad de Artes Liberales, Univ. Adolfo Ibáñez, Viña del Mar, Chile. BRB also at: Instituto Milenio en Socio-Ecologia Costera (SECOS) & Núcleo Milenio UPWELL.

Oikos
00: 1–14, 2021
doi: 10.1111/oik.08267

Subject Editor: Matthew Bracken
Editor-in-Chief: Dries Bonte
Accepted 14 May 2021

Improving our understanding of stability across spatial scales is crucial in the current scenario of biodiversity loss. Still, most empirical studies of stability target small scales. We experimentally removed the local space-dominant species (macroalgae, barnacles, or mussels) at eight sites spanning more than 1000 km of coastline in north- and south-central Chile, and quantified the relationship between area (the number of aggregated sites) and stability in aggregate community variables (total cover) and taxonomic composition. Resistance, recovery, and invariability increased nonlinearly with area in both functional and compositional domains. Yet, the functioning of larger areas achieved a better, albeit still incomplete, recovery than composition. Compared with controls, smaller disturbed areas tended to overcompensate in terms of total cover. These effects were related to enhanced available space for recruitment (resulting from the removal of the dominant species), and to increasing beta diversity and decaying community-level spatial synchrony (resulting from increasing area). This study provides experimental evidence for the pivotal role of spatial scale in the ability of ecosystems to resist and recover from chronic disturbances. This knowledge can inform further ecosystem restoration and conservation policies.

Keywords: disturbance, habitat fragmentation, invariability–area relationship, marine protected areas, perturbation

NORDIC SOCIETY OIKOS

www.oikosjournal.org

Introduction

Ecological stability describes the ability of populations, communities, and ecosystems to resist and recover from natural and anthropogenic disturbances (Grimm and Wissel 1997). Anthropogenic disturbances act on a broad range of spatial scales, but to date, empirical studies on community stability have been conducted mostly at local scales (Kéfi et al. 2019). Importantly, realising biodiversity loss and ecosystem stability at the scales of landscapes and regions is critical for ecosystem management (Isbell et al. 2017). Such a lack of congruence between the spatial scale of stability research and ecosystem processes seriously limits our ability to make sustainable conservation decisions to abate global biodiversity crisis (Gonzalez et al. 2020). Therefore, it is key to improve our understanding of how stability scales from local to regional spatial scales.

At large spatial scales, stability may be regulated by the spatial variation in species composition – beta diversity (Whittaker 1972) – in addition to species evenness, environmental correlation, and dispersal (Lande et al. 1999, Loreau et al. 2003, France and Duffy 2006). When functioning is calculated as a community-level aggregate property, such as biomass or cover, beta diversity has a negative effect on the spatial synchrony of this property among communities (i.e. community-level spatial synchrony; Fig. 1): assuming that species from different functional types have different effects on functioning, a high beta diversity will ensure that different local communities have different temporal patterns of the aggregate property (Loreau et al. 2003, Wang and Loreau 2014). Consequently, such spatial differences diminish the temporal variation in the aggregate property or function when subsumed at the regional scale – i.e. increase invariability (Wang et al. 2019).

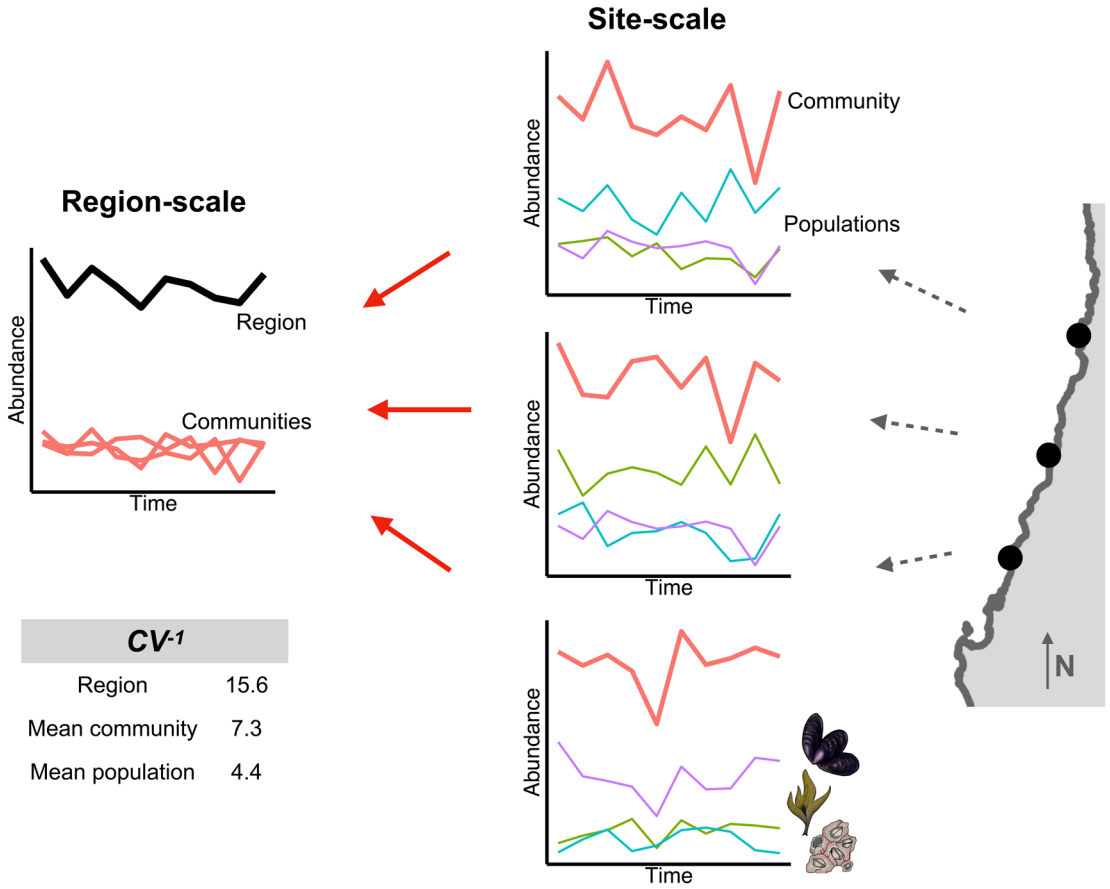

Figure 1. Scheme of the temporal variation and synchrony in abundance of a theoretical marine intertidal region. At the site-scale, the three local communities have different compositions, defined as the combination of species occurrences and abundances: While the community at the northern site is dominated by barnacles (cyan lines in the right panels), the central community is dominated by macroalgae (green lines) and the southern community by mussels (purple lines). Total community abundance (e.g. biomass or cover, red lines) at each site is defined as the sum of abundances across species populations and represents an aggregate community-level function. At the regional scale, total abundance (black thick line in the left panel) is the sum of all community-level abundances. Community-level spatial synchrony describes the positive correlation among the temporal fluctuations of communities' abundances in the region. In this way, the spatial variation in composition, beta diversity, in this region is associated with asynchronous community-level fluctuations and more 'stable' (less variable) temporal fluctuations across spatial scales (lower left table). CV^{-1} is the inverse coefficient of variation of the aggregate function (Tilman 1999). Species illustrations by Fundación Mar y Ciencia.

Invariability is the degree of constancy in an aggregate function (or composition) over time and can be estimated, for example, as the inverse of the temporal coefficient of variation of that property (Grimm and Wissel 1997, Tilman 1999). If the temporal patterns in functioning of the different local communities become more different at larger spatial scales (i.e. the community-level spatial synchrony decreases), then a positive invariability–area relationship can be observed: the aggregate community property becomes more stable over time when examined over larger spatial scales (Wang et al. 2019). Recent empirical work provides support for positive and nonlinear invariability–area relationships (Gonzalez et al. 2020). For instance, Wang et al. (2017) demonstrated the existence of a quasilinear increase of invariability with increasing area for bird biomass in eastern North America, where area was expressed as the number of survey routes. In a more general framework of ecological hierarchies, the number of elements in lower levels is expected to boost the invariability of higher levels of the hierarchy (Jørgensen and Nielsen 2013). Thus, increasing the number of communities can be predicted to increase stability, measured as invariability in a given ecosystem function (Wang and Loreau 2014).

Invariability is, however, one of the several dimensions of stability (Pimm 1984, Donohue et al. 2013, Kéfi et al. 2019). These dimensions also include, but are not limited to, the degree to which the ecological system remains unchanged after a disturbance (resistance), the speed of the recovery after the disturbance (Pimm's resilience and later Holling's engineering resilience), and the degree to which the system achieves pre-disturbance levels (recovery; Pimm 1984, Holling 1996, Grimm and Wissel 1997). Despite theoretical work describing associations among some dimensions of stability (Harrison 1979, Scheffer et al. 2009, Donohue et al. 2013), recent empirical and modelling studies demonstrate that these correlations span the range from negative to neutral to positive (Hillebrand et al. 2018, Radchuk et al. 2019), which can complicate the analysis of the spatial scaling of stability. Another important consideration is that each of these dimensions can be expressed in terms of an aggregate, community-level function (i.e. functional stability) or in terms of the variation in species identities and abundances (compositional stability; Micheli et al. 1999). Understanding the spatial scaling of stability requires the analysis of both domains, because they may well be uncorrelated depending on the ability of different species to perform similar functions (Tilman 1996, Guelzow et al. 2017). Thus, besides functional invariability, how do different stability dimensions and domains vary with spatial scale? Peterson et al. (1998) proposed a hierarchical model where higher functional diversity in larger regions leads to greater compositional resilience (Holling 1973, Peterson et al. 1998). To the best of our knowledge, however, the analysis of multiple stability dimensions across spatial scales is still incipient (Clark et al. 2021).

Here, we examine the spatial scaling of four stability dimensions in a field manipulative experiment replicated in multiple sites spanning ca 1000 km of the southeastern Pacific coast. The experiment involved the repeated removal of individuals belonging to several sessile species that dominate primary space. This allowed us to evaluate changes in functional (total cover) and compositional (species identities and abundances) stability. For assemblages of sessile species, total cover represents the outcome of disturbance and competition for space as a limiting resource (Paine 1980), where the vast majority of space-dominant and subdominant species must receive propagules from the regional larval pool (Roughgarden et al. 1988, Menge et al. 2015). By pooling data from different numbers of sites (two to eight), we used the number of sites as a proxy for ecosystem area. In this region, the removal of the locally dominant species (i.e. the corticated red alga *Mazzaella laminarioides*, chthamalid barnacles, or the purple mussel *Perumytilus purpuratus*) have been shown to cause stability responses that are very similar in magnitude across sites (Valdivia et al. 2021a). This similarity was observed between sites clustered at the northern and southern extremes of the entire region, despite large environmental differences among sites, and despite morphological, functional, and phylogenetic differences among the three locally dominant species. The experiment was used to test two interrelated hypotheses:

1. H1. Community-level spatial synchrony decreases with area

   This prediction is based on the assumption that beta diversity increases with increasing area due to, for example, enhanced environmental heterogeneity and niche opportunities (Fukami et al. 2001, Barton et al. 2013, Vellend 2016). Beta diversity, in turn, is expected to reduce the spatial synchrony in community functioning (Wang et al. 2019).

2. H2. Each dimension of functional and compositional stability increases nonlinearly with area

   As local communities coalesce into larger areas, the reduced community-level spatial synchrony allows the different communities to compensate each other over time (i.e. a spatial analogue of the insurance effect; Loreau et al. 2003). This, in turn, is expected to increase overall resistance, resilience, recovery, and invariability in both functioning and composition.

Methods

Study region

Rocky intertidal habitats provide an opportunity to test ecological responses to disturbances across spatial scales. Short generation times, small body sizes, and the functional and taxonomic diversity that characterise intertidal communities in temperate zones allow experimental manipulations to be carried out over meaningful spatiotemporal scales of observation (Bracken et al. 2017). The study was conducted in eight sites, equally distributed at the equator- and poleward extremes of

a large coastal biogeographic province along the south east Pacific (ca 30°S and 40°S, respectively; Fig. 2). The province is the transition between the Peruvian and Magellan provinces (Camus 2001, Thiel et al. 2007, Lara et al. 2019). Each subregion included four sites and spanned ca 200 km of the shoreline (Fig. 2). The sessile communities of the mid rocky intertidal zone are characterised by a diverse assemblage that is locally dominated by opportunistic macroalgae like *Ulva rigida* and *U. compressa*, corticated macroalgae like *Mazzaella laminarioides* and *Gelidium chilense*, or filter feeders like the barnacles *Jehlius cirratus*, *Notochthamalus scabrosus,* and the purple mussel *Perumytilus purpuratus* (reviewed by Aguilera et al. 2019).

This study was based on a multi-scale experimental design: The record was the basic unit of estimation of the abundance (percentage cover) of a species in a sample. The sample encompassed the data of all records belonging to the same sampling event of a plot that had a fixed location on the shore. Since each plot was repeatedly sampled over time, then all these samples belonged to the same plot. Multiples plots, assigned to either the dominant removed or control treatment, were nested within each site (see the Supporting information, details of within-site plot replication in the Experimental design and setup section). The region encompassed the highest observation unit in the study and was defined by groups of randomly aggregated sites; each group was composed by two to eight sites. Before the analyses, the data of all plots were averaged for each treatment and site separately for each sampling date. Thus, site and region were the spatial scales analysed in the study.

Experimental design and setup

At the mid intertidal zone of each site, we conducted a manipulative experiment where the removal of the locally dominant sessile species was a fixed factor. The experiments were conducted between October 2014 and August 2017 in the southern subregion, and between December 2014 and September 2017 in the northern subregion. All observations and experimental manipulations were carried out during diurnal low tide hours (tidal range ca 1.5 m). To determine the locally dominant species in each site, we estimated relative species abundances in ten 30 × 30 cm plots haphazardly located within a 3 × 50 m alongshore transect. The species with the highest relative abundances at each site were considered as locally dominant (Rius et al. 2017). *Mazzaella laminarioides* and chthamalid barnacles (a mixture of *J. cirratus* and *N. scabrosus*) were the dominant taxa in the northern subregion; chthamalid barnacles and *P. purpuratus* were the dominant species in the southern subregion. At sites LIMA and PTAL (Fig. 2), *M. laminarioides* dominated with abundances between 20% and 65% (plot-scale 1st and 3rd quantiles, respectively); at TEMB, GUAN, and CHAI, barnacles dominated with abundances between 26% and 69%; at CHEU, CALF, and PUCA, *P. purpuratus* dominated the communities with abundances between 98% and 100% (Valdivia et al. 2021a).

The field experiments included, as experimental units, 30 × 30 cm plots located on the mid-intertidal zone and within areas of high abundance of the locally dominant species. Each plot was permanently marked with stainless-steel bolts. Ten replicate plots were located in the northern part of the region and 20 replicates in the southern part. Experimental plots were haphazardly located in areas that excluded crevices, tide-pools, and vertical surfaces to reduce biotic variation related to local spatial heterogeneity.

At the start of the experiment (i.e. between October and December 2014 in the southern and northern subregions, respectively), each plot was randomly assigned to one of two groups: either dominant removed or control. Half of the plots in each site were assigned to each group. The species dominating each site was completely removed from each dominant removed plot with scrapers and chisels. The control plots remained unmanipulated. Settlers and recruits of the dominant species were further removed from the dominant removed plots approximately every three months; i.e. a press disturbance treatment (Bulleri et al. 2012).

The abundance of each macrobenthic species (> 5 mm) was estimated in each plot immediately before the removal of local dominants, 1–2 months after, and then approximately every three months until the end of the experiment. All macroalgae and sessile macroinvertebrates in each plot were identified in situ and classified to the lowest possible taxonomic level (usually species). Sessile species abundances were estimated as percentage covers (1% resolution). To this aim, we used a 0.09-m^2 frame divided in 25 equal fields with a monofilament line. The organisms growing on both primary and secondary substrata (i.e. rock and other organisms, respectively) were quantified, which allowed total community cover to exceed 100%.

The data obtained during the 11 successive surveys conducted after the first removal were used to estimate beta diversity, community-level spatial synchrony, and four dimensions of stability (resistance, resilience, recovery, and invariability) separately for the functional and compositional domains. Since we were interested in the response of the remaining community to the local extinction of dominants, the latter were removed from the dataset when we assessed beta diversity, community-level spatial synchrony, and stability.

Spatial scaling of communities

To assess the relationship between the scale of observation and stability, individual sites (n = 8) were aggregated into groups of cumulative numbers of communities. This method resembled the aggregation of sites or samples in a species-accumulation curve, where the curve is defined by the mean species richness under all possible permutations of samples (Ugland et al. 2003). Accordingly, area (A) was expressed as the number of sites included in the calculation of the stability dimensions and domains. Area varied, therefore, from two to eight pooled sites. Beta diversity, community-level spatial synchrony, and each stability dimension within the functional and compositional domains were calculated for

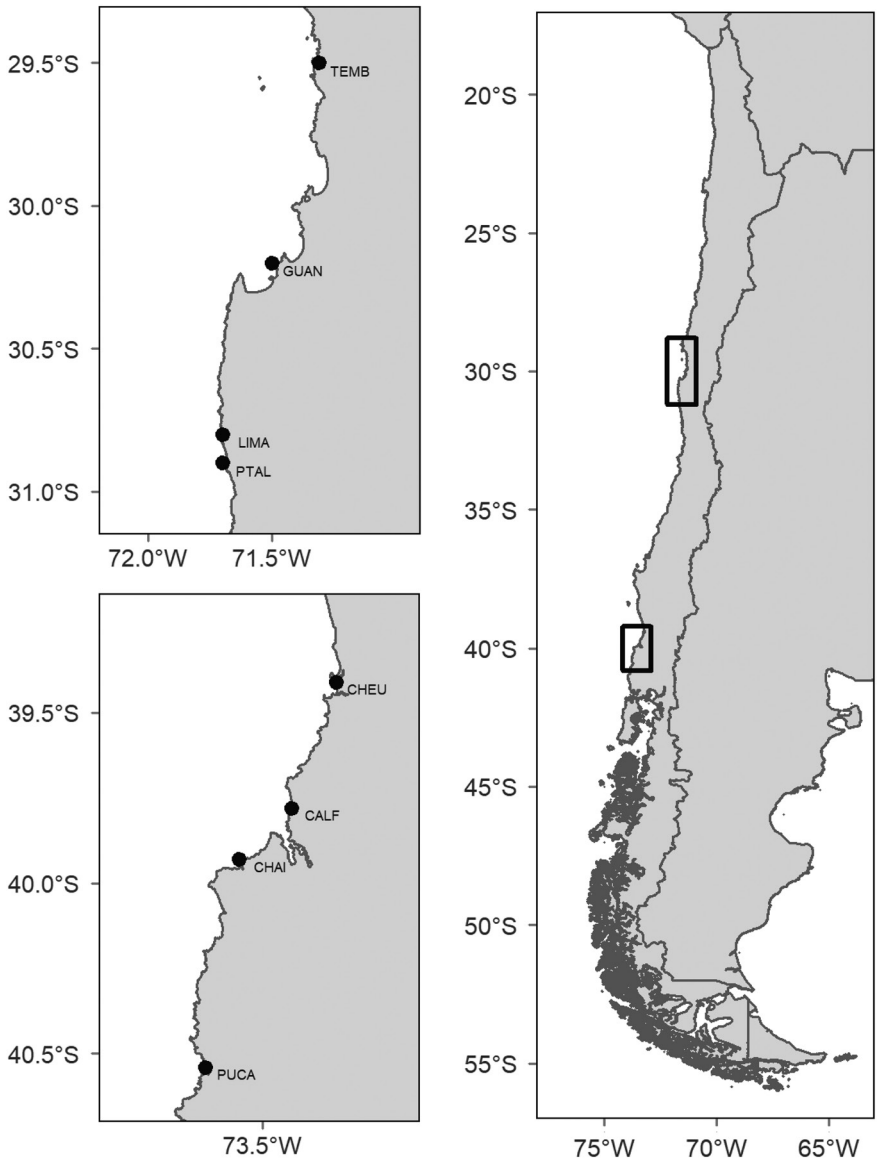

Figure 2. Study intertidal sites at both extremes of a biogeographic transitional province on the southeastern Pacific shore. Site codes are TEMB: Temblador, GUAN: Guanaqueros, LIMA: Limarí, PTAL: Punta Talca, CHEU: Cheuque, CALF: Calfuco, CHAI: Chaihuín, and PUCA: Pucatrihue.

each permutation of sites. To test for potential artifacts due to grouping sites from distant shore subregions (Fig. 2), we conducted the analyses with and without combining the local communities at the extremes of the region. The analyses of the reduced dataset yielded qualitatively similar results to those from the entire dataset, but with increased unexplained variance (Supporting information). For brevity, here we present the results of the entire dataset, combining both shore sub-regions.

Beta diversity and community-level spatial synchrony

Beta diversity was estimated as the between-site Jaccard dissimilarities for each combination of sites and separately for removal and control conditions. Jaccard dissimilarity quantifies between-site pairwise differences in species occurrences as: $D = 1 - \frac{A_s}{A_s + B_s + C_s}$, where D is the distance-transformed Jaccard's coefficient, A_s is the number of species occurring at both sites, B_s is the number of species occurring only at one site, and C_s is the number of species occurring only at the other site (Jaccard 1900, Legendre and Legendre 1998). In this way, Jaccard dissimilarity ranges between zero and one (both sites share the same species or do not share any species, respectively). For this estimation, species abundances were averaged over time before transforming them to presence–absence data. The removal of the dominant species could have enhanced the available surface for recruitment. A larger area devoid of organisms could have increased Jaccard's

dissimilarity, which can be more sensitive to differences in sample effort than metrics based on species abundances (Beck et al. 2013). Therefore, this analysis was further complemented with abundance-based beta diversity, calculated as: $D_{BC} = 1 - \frac{W}{A_a + B_a}$, where D_{BC} is the Bray–Curtis dissimilarity, W is the sum of the minimum abundances across species, and Aa and Ba are the sum of abundances at each of both sites under comparison (Odum 1950, Legendre and Legendre 1998).

The community-level spatial synchrony was calculated as: $\varphi_C = \frac{\sqrt{v_{\Sigma,\Sigma}}}{\sum_k \sqrt{v_{\Sigma,kk}}}$, where $v_{\Sigma,\Sigma}$ is the temporal variance of the whole regional cover and $\sum_k \sqrt{v_{\Sigma,kk}}$ is the summed site-specific standard deviations of community cover (Wang et al. 2019). This metric ranges from zero, expressing perfectly desynchronised temporal fluctuations in community cover, to one, representing perfectly synchronised fluctuations among sites. We used the *var.partition* R function (Wang et al. 2019) to calculate community-level spatial synchrony, which was calculated separately for the removal and control conditions, and each combination of sites.

Stability dimensions and domains

Resistance, resilience, recovery, and invariability were estimated as described by Hillebrand et al. (2018). Stability metrics in the functional domain were calculated for total regional cover (*F*). For the compositional domain (i.e. species composition), we modified the original formulation of Hillebrand et al. (2018) by using Bray–Curtis dissimilarities (*dis*) rather than similarities between the disturbed and control conditions. In this way, values of zero for resistance and recovery indicated maximum stability for both function and composition.

Resistance (*a*) was estimated for function as the log-response ratio (*LRR*) calculated after the disturbance took place (1–2 months after the removal of local dominants): $a = \ln\left(\frac{F_{dist}}{F_{con}}\right)$, where F_{dist} and F_{con} are the total percentage cover of the dominant-removed and the control conditions, respectively. A value of $a = 0$ indicates maximum resistance of the community to the disturbance and $a < 0$ and $a > 0$ indicate low resistance due to under- and overperformance relative to controls, respectively (Hillebrand et al. 2018).

The resistance of composition (*a*) was calculated on the basis of Bray–Curtis dissimilarities between the disturbed and the control conditions: $a = dis\left(\frac{C_{dist}}{C_{con}}\right)$, where C_{dist} and C_{con} are the species-abundance matrices in the dominant-removed and control areas, respectively after the disturbance took place. Minimum dissimilarities of $a = 0$ indicate 100% of similarity between disturbed and control conditions and thus maximum resistance. Maximum dissimilarities of $a =$ indicate 0 % of similarity between both conditions and thus extremely low resistance.

Resilience (*b*) was calculated as the slope of the linear regression of *LRR* and *dis* calculated for each sampling event (Hillebrand et al. 2018): $\ln\left(\frac{F_{dist}}{F_{con}}\right) = i + b*\mathrm{t}$, and $dis\left(\frac{C_{dist}}{C_{con}}\right) = i + b*\mathrm{t}$, where *i, b,* and t are the intercept, slope, and time, respectively. A *b*-value equalling zero indicates no change over time. For functioning, $b > 0$ and $b < 0$ indicate a faster recovery and further deviation from control, respectively, when resistance is negative (underperformance relative to control); if functional resistance is positive (overperformance), then $b > 0$ and $b < 0$ indicate a further deviation from control and a faster recovery, respectively. For composition, $b > 0$ and $b < 0$ indicate a further deviation from control and a faster recovery, respectively.

Recovery (*c*) was estimated as the *LRR* and *dis* calculated at the end of the experiment. For functioning, $c = 0$ denotes maximum recovery, $c < 0$ incomplete recovery, and $c > 0$ overcompensation with respect to the control condition. For composition, $c = 0$ and $c > 0$ denote maximum recovery and incomplete recovery, respectively.

Invariability (*d*) was calculated as the multiplicative inverse of the standard deviation of residuals (*resid*) from the regression slope *b* as $d = \left(\frac{1}{sd\left(resid_b\right)}\right)$. Larger *d* values denote smaller temporal variations around the trend of recovery in function or composition (Hillebrand et al. 2018, Radchuk et al. 2019).

Statistical analyses

Beta diversity and community-level spatial synchrony (φ_c) were analysed using weighted generalised linear models (GLM). Since both response variables were bound between zero and one, we assumed a beta distribution of errors and log link for both models. The models included area (*A*) and dominant species removal as fixed and crossed effects. In addition, the models included the average Euclidean between-site distance as explanatory variable. An orthogonal second-order polynomial contrast was used for *A* to account for nonlinear patterns. The data of *A* were centred around the mean (between four and five sites) to set the model intercept at this point rather than an unrealistic area of zero sites. Model parameters were estimated through maximum likelihood. A pseudo-R^2, based on the squared correlation of the linear predictor and link-transformed response, was used as goodness of fit (Ferrari and Cribari-Neto 2004).

The stability–area relationship was modelled for each stability dimension and within each domain (functional and compositional) with nonlinear quantile least-squares regressions. We chose quantile regressions to account for large variability observed for small-sized metacommunities and

to describe both positive and negative values of the stability metrics. 95%, 50% and 5% quantiles were analysed to represent maximal, median, and minimal stability responses, respectively. To each dimension and quantile, we fitted a power-law model in the form of $S = c_1 A^z$, where S is the stability dimension, c_1 the intercept, and z the scaling exponent.

Since the number of community combinations, and thus the variance, varied among the levels of A, we used variance $(y)^{-1}$ as weights in the models of beta diversity and φ_c. Weights were not necessary in the models for stability dimensions, as they were analysed with quantile regressions. Graphical exploration of residuals and fitted values were used to corroborate the effectiveness of weights and as model diagnostics. In this study, we used the *betapart, betareg, cowplot, quantreg, tidyverse, tmap* and *vegan* R packages (Gruen et al. 2012, Wilke 2016, Baselga et al. 2018, Tennekes 2018, Oksanen et al. 2019, Wickham et al. 2019, Koenker 2020, <www.r-project.org>).

Results

Beta diversity (Jaccard's D) increased nonlinearly with increasing area A (Fig. 3A, Table 1, pseudo-$R^2 = 0.47$, linear and quadratic coefficients of controls = 43.8 and 0.44, respectively). The removal of the dominant species positively affected beta diversity of all areas, except those composed by two sites (Fig. 3A, Table 1, linear and quadratic coefficients of disturbed regions = 16.47 and 0.5, respectively). Geographic distance was positively associated with beta diversity, albeit this association was comparatively small (Table 1; coefficient for area = 1.03). Abundance-based beta diversity (Bray–Curtis dissimilarities) exhibited a nonlinear increment with area, and a positive response to the removal of dominant species; however, the between-treatment difference in Bray–Curtis was minor when compared with Jaccard (Supporting information). Community-level spatial synchrony (φ_c) decayed as A increased, and this pattern was steeper for disturbed than control areas (Fig. 3B, Table 1, pseudo-$R^2 = 0.28$, linear and quadratic coefficients of controls = 0.21 and 1.65, respectively; and of disturbed regions = 0.1 and 1.77, respectively).

Area exhibited nonlinear effects on the functional and compositional stability dimensions. The maximum values of functional resistance strongly increased (approached zero) with increasing A (Fig. 4A), which was supported by a statistically significant scaling coefficient for the 95% quantile (z = −0.74, Table 2). While the median (50%) did not vary, the minimal functional resistance (5%) significantly increased across A (approached zero; z = −3.11 for the 5% quantile, Table 2). For most regions, therefore, dominant removal triggered an increase in function (i.e. overperforming relative to controls; Supporting information). Resilience in the functional domain decreased with increasing A, as smaller regions changed faster after the disturbance started (Fig. 4B). This pattern was supported by the statistically significant fits of the non-linear model on maximal and minimal functional resilience – both quantiles approached zero with increasing A (z = −1.65 and −0.75, respectively, Table 2). Maximal functional recovery increased (i.e. approached zero) with increasing A (Fig. 3C; z = −0.83, Table 2), indicating that larger regions achieved a better recovery than smaller ones. However, and irrespective of the area, most of the disturbed regions did not fully recover, overcompensating in functioning relative to controls by the end of the experiment (Fig. 4C). Finally, functional invariability exhibited

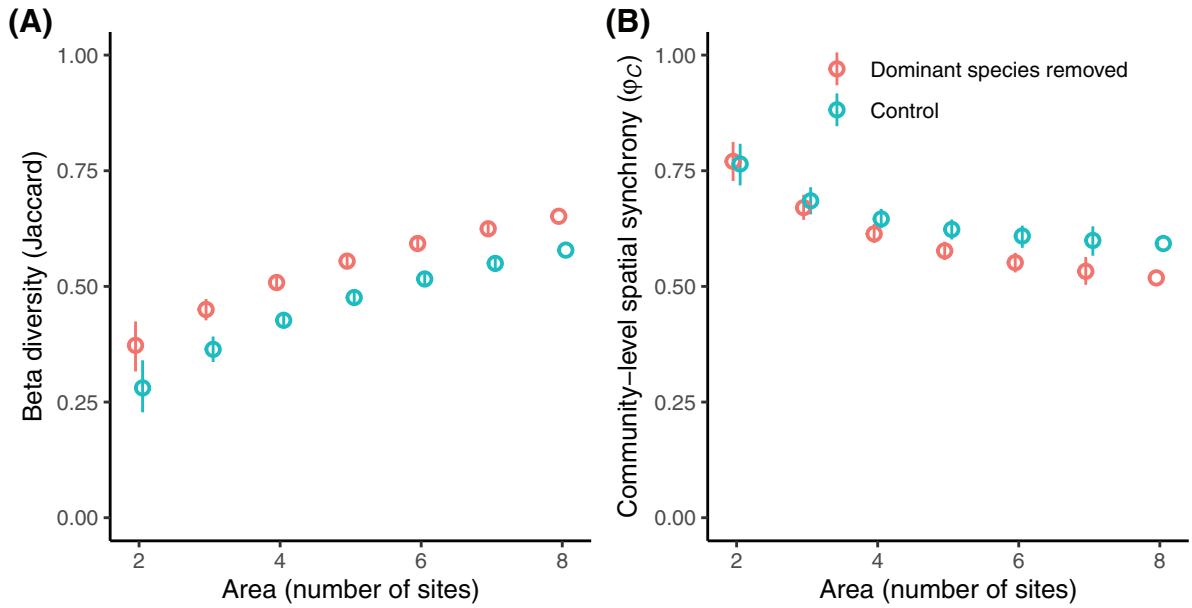

Figure 3. Beta diversity (Jaccard dissimilarities, panel A) and community-level spatial synchrony (φ_C, panel B) across areas. Values are provided as means ± 95% confidence intervals.

Table 1. Parameters of generalised linear models (beta distribution of errors and log link) for the separate and interactive effects of area (*A*), the experimental removal of locally dominant species (R), and geographic distance (*Distance*) on beta diversity (*D*) and community-level spatial synchrony (φ_C). Orthogonal polynomial contrasts were used for *A* (linear and quadratic, A_L and A_Q, respectively). The parameters and SE were back-transformed from the ln scale. Thus, a value of 1 indicates no effect, < 1 a negative effect, and > 1 a positive effect.

Response	R^2	Parameter	Estimate	SE	z
Beta diversity (*D*)	0.50	*Intercept*	0.42	1.001	−1002.7
		A_L	43.76	1.021	184.2
		A_Q	0.44	1.015	−55.6
		Removal (Re)	1.21	1.001	167.6
		Distance	1.03	1.001	44.5
		Re:A_L	0.38	1.027	−36.8
		Re:A_Q	1.33	1.019	14.8
Community-level spatial synchrony (φ_C)	0.26	*Intercept*	0.66	1.001	−567.7
		A_L	0.22	1.015	−102.0
		A_Q	1.65	1.014	35.7
		Re	0.95	1.001	−47.9
		Distance	0.97	1.001	−55.2
		Re:A_L	0.48	1.022	−34.5
		Re:A_Q	1.09	1.021	4.0

R^2, pseudo coefficient of determination; SE, standard error of the parameter; z, test statistic. For each parameter, the probability of observing the statistic or larger by chance (p-value) was < 0.001.

a saturating increase with *A*, in particular for the median and minimum values (Fig. 4D; z = 0.21 and 0.5, respectively, Table 2).

Compositional resistance largely varied with increasing *A* (Fig. 5A). While maximal and median compositional resistance approached zero, minimal compositional resistance further departed from zero as *A* increased (−0.17, −0.11, and 0.41, respectively, Table 2). Minimal compositional resilience approached zero with increasing *A* (Fig. 5B; z = −0.74, Table 2). For compositional recovery, we observed that both maximal and median values approached zero (i.e. increased), while minimal values departed from zero (i.e. decreased) along area – the disturbed regions did not achieve a full recovery by the end of the study (Fig. 5C; z = −0.29, −0.12 and 0.38 for 95%, 50% and 5%, respectively, Table 2). Lastly, median and minimal compositional invariability increased nonlinearly with increasing *A* (Fig. 5D; z = 0.31 and 0.35, respectively; Table 2).

Discussion

Understanding how stability varies across spatial scales is key to counteract global biodiversity crisis. Here, we have demonstrated empirically that different dimensions of stability in spatially extended regions are scale dependent. As expected, beta diversity increased, and the community-level spatial synchrony decayed, with spatial scale. This result reflects the role of spatial biological complexity in ensuring that different local communities have different temporal patterns of functioning. The removal of dominant species elicited an increase in functioning and alteration of composition, effects that were particularly stronger for most of the smaller areas. Functional and compositional resilience (i.e. velocity of the recovery trajectories) were faster in smaller than larger areas. However, larger areas achieved a fuller, yet incomplete, recovery than smaller areas, which further departed from the controls in terms of functioning and composition. Functional and compositional invariability exhibited a positive and saturating pattern with area. Our assessment of several stability dimensions provided a comprehensive understanding of the spatial scaling of ecological responses to a common disturbance (i.e. the local extinction of dominant species), which could be driven by natural or anthropogenic mechanisms.

Beta diversity and community-level spatial synchrony responded to changes in area

The increase in beta-diversity with area is most likely explained by the larger environmental heterogeneity accrued with area and the enhanced niche availability and thus niche complementarity that can be observed in larger regions (Chesson 2000, Vellend 2016). The study region encompasses a mosaic of oceanographic conditions associated with semipermanent upwelling activity in the north and frequent riverine inputs in the south (Broitman et al. 2001, Lara et al. 2019). For instance, upwelling activity mediates large variations in sea surface temperature along the southeastern Pacific shore (Hormazabal et al. 2004, Garreaud et al. 2011, Pinochet et al. 2019), which could well offer different niche conditions for coastal species. On the other hand, upwelling activity and riverine inputs also curtail the arrival of juvenile and planktonic propagules of coastal species, strongly contributing to spatial differences in species composition in our study region and elsewhere (Morgan et al. 2009, Fenberg et al. 2015, Lara et al. 2019). Indeed, low dispersal (leading to recruitment limitations) is predicted to boost spatial beta diversity, independent of competition or abiotic niche breadths (Thompson et al. 2020). In the northern extreme of the region, observational evidence suggests that the joint effects of local abiotic environmental conditions and recruitment limitations account for most of the spatial variation in community structure of

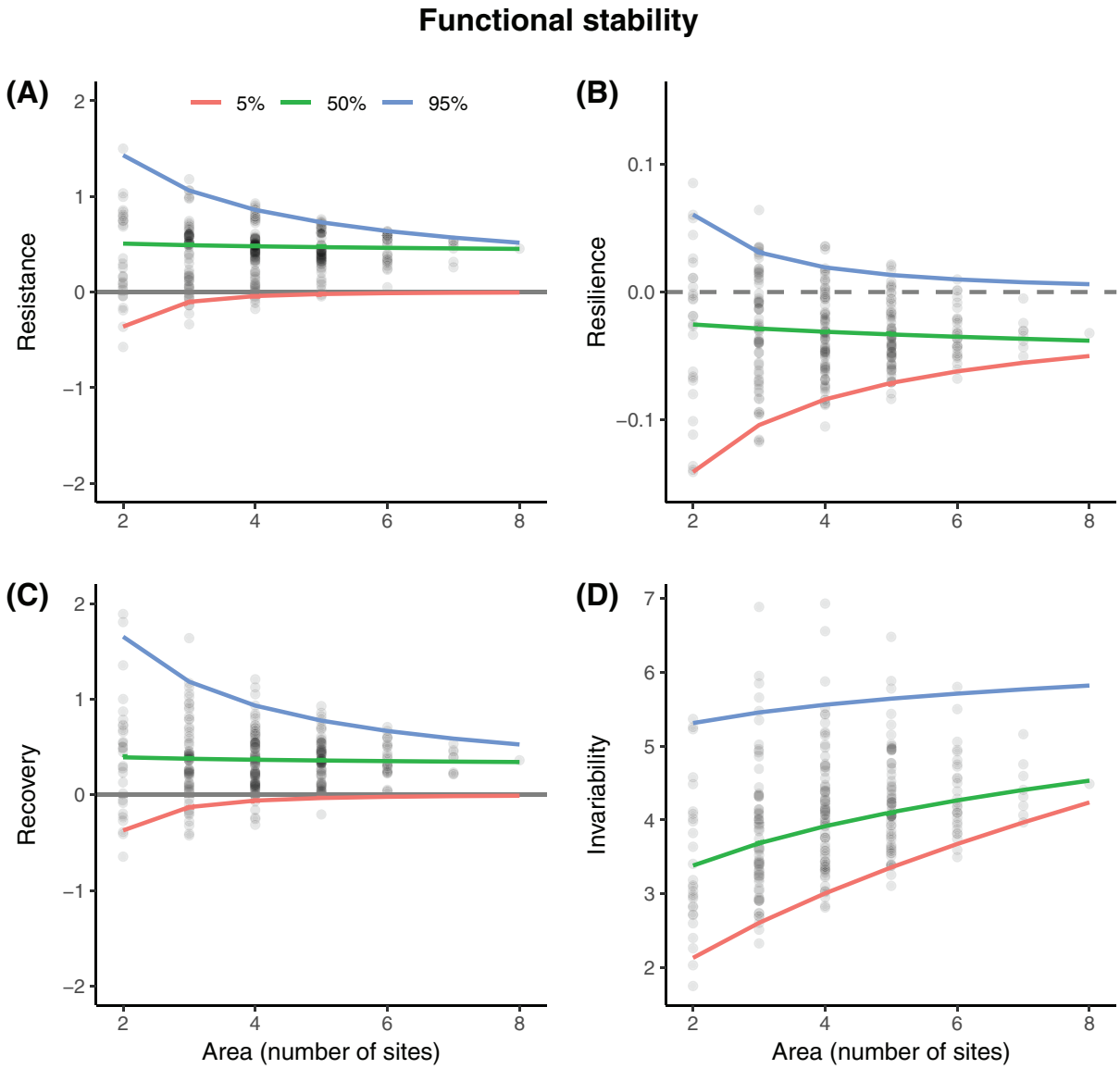

Figure 4. Spatial scaling of four dimensions of the stability in total cover in response to the experimental removal of the locally dominant species. The horizontal continuous grey line indicates maximal stability for resistance and recovery. The horizontal dashed grey line denotes minimal resilience. Blue, green, and red lines represent the predicted values of quantile nonlinear models for the 95%, 50% and 5% quantiles, respectively.

rocky intertidal sessile organisms (Valdivia et al. 2015). In our study, the strong mesoscale (10 s to few 100 s of km) variation of these coastal processes might account for the comparatively low effect of geographic distance per se on beta diversity when broader spatial scales were analysed.

Increased beta diversity following the removal of the locally dominant species agrees with evidence from other ecosystems (Hyman et al. 2019). Since dominant species covered a large proportion of the substratum (up to 100% of some plots), their removal released a significant amount of space available for colonisation and vegetative growth of subordinate organisms. This would have contributed to the increased, relative to controls, beta diversity of disturbed areas. The stronger disturbance effect on incidence- than abundance-based beta diversity supports the role of the available space in driving the spatial variation in composition (Beck et al. 2013). Alternatively, the loss of facilitative interactions would also explain part of the effect of the removal of the dominant species on beta diversity. Enhanced survival and reproduction of numerically dominant sessile species is followed by larger and more homogenous aggregations of individuals (Dunstan and Johnson 2006, Wilsey et al. 2014, Rius et al. 2017). The ability of many dominant species to enhance habitat structural complexity results in habitat provision for subordinate and transient species, altering their settlement and abundance patterns (Jones et al. 1994, Eriksson et al. 2006). This facilitative interaction is particularly relevant in stressful environments – like the mid rocky intertidal (Bruno et al.

Table 2. Scaling coefficients (z) of quantile nonlinear regression models for four stability dimensions (resistance, resilience, recovery, and invariability) as functions of area. We fitted a power-law function to each stability dimension as $S_i = c_i A^z$, where S_i is the stability dimension i and A is area (number of sites). 95%, 50% and 5% quantiles of each dimension were analysed separately.

		Function				Composition			
Dimension	Quantile (%)	z	SE	t	p	z	SE	t	p
Resistance	95	−0.74	0.14	−5.41	<0.001	−0.17	0.03	−5.21	<0.001
	50	−0.08	0.26	−0.32	0.752	−0.11	0.04	−2.59	0.010
	5	−3.11	1.50	−2.07	0.039	0.41	0.14	2.97	0.003
Resilience	95	−1.65	0.57	−2.92	0.004	−0.50	0.34	−1.46	0.146
	50	0.29	0.31	0.96	0.340	0.43	0.42	1.04	0.300
	5	−0.75	0.11	−6.56	<0.001	−0.74	0.24	−3.04	0.003
Recovery	95	−0.83	0.18	−4.55	<0.001	−0.29	0.05	−5.36	<0.001
	50	−0.10	0.24	−0.41	0.684	−0.12	0.06	−2.16	<0.001
	5	−2.63	1.80	−1.46	0.147	0.38	0.06	6.30	0.032
Invariability	95	0.07	0.07	0.92	0.360	0.12	0.13	0.94	0.347
	50	0.21	0.06	3.45	0.001	0.31	0.06	5.23	<0.001
	5	0.50	0.06	7.76	<0.001	0.35	0.08	4.61	<0.001

SE, standard error of the parameter; t, test statistic; p, probability of observing the statistic or larger by chance.

2003) – which can further reduce beta diversity (Jurgens and Gaylord 2018).

The effect of dominant removal on beta diversity responded to both increased and decreased abundances of subordinate species. For instance, the removal of the purple mussel *Perumytilus purpuratus* boosted de populations of green algae (Ulvoids) during the first year of the experiment, which were replaced by barnacles over time in most of the southern sites (Valdivia et al. 2021a). On the contrary, the removal of barnacles in the most equatorialward site, TEMB, caused a decrement in the abundance of Ulvoids and an increment in that of *Pyropia* spp. (Valdivia et al. 2021a). These results suggest that both, release of recruitment space and weakening facilitative interactions could have driven the response of beta diversity to the experimental extirpation of space-dominant species.

Beta diversity responses were associated with systematic reductions in community-level spatial synchrony. This result is in agreement with spatial models where biological complexity represents a spatial insurance that allows for between-site compensatory dynamics (Loreau et al. 2003, Wang et al. 2019). Since spatial synchrony in aggregate properties is central for region-scale stability, our results provide empirical evidence supporting spatially explicit management strategies against rampant biotic homogenisation (Isbell et al. 2017, Mori et al. 2018).

Stability increased with area

Recent theoretical advances in the scale-dependency of stability and ecosystem functioning (reviewed by Gonzalez et al. 2020) agree with our findings that increased beta diversity and reduced community-level spatial synchrony were followed by concomitant increases in recovery and invariability. Most of the smallest areas exhibited a large departure from controls in terms of functioning and composition. Both functional and compositional resilience diminished (approached zero) nonlinearly as area increased. Thus, the function and composition of smaller areas varied faster over time than those of larger areas. The smaller areas, however, exhibited a more incomplete recovery (i.e. farther from zero) by the end of the study, suggesting that they further departed from the reference condition. Indeed, most of the smaller disturbed areas overcompensated in functioning (relative to controls) by the end of the study, which could well be related with increased available space upon the removal of the dominant species. In this context, Peterson et al. (1998) suggest that the distribution of functional groups within and across spatial scales mediates the stability of ecological communities – specifically, the redundancy of functional types across scales can improve compositional recovery after disturbances. Thus, the spatial scaling of both taxonomic and functional diversity shall account for the resistance, resilience, and recovery of the larger regions in this study (Delsol et al. 2018). However, species richness seems to be less relevant for stability than species-level synchrony in the northern subregion of the studied biogeographic province (Broitman et al. 2011, Valdivia et al. 2013). A recent global meta-analysis demonstrated that, at least for terrestrial primary producers, species asynchrony accounts for a larger amount of variation in community-level stability than species richness (Valencia et al. 2020). Although that work analysed only invariability, earlier models emphasised that different dimensions of stability need to be assessed in the context of multiple factors affecting local communities, and not only species diversity (Ives and Carpenter 2007).

An important result of this study was the observed invariability–area relationships for both function and composition, which were well explained by a power law function. These curves were similar to the large-scale section of the quasilinear invariability–area relationship described for North American bird community biomass (Wang et al. 2017). In that study, the authors used the number of bird sampling routes as a proxy for area. Albeit our method of grouping local sites to resemble different areas allowed us to detect a notable invariability–area relationship, this association could well adopt different shapes, such as the triphasic trend described for

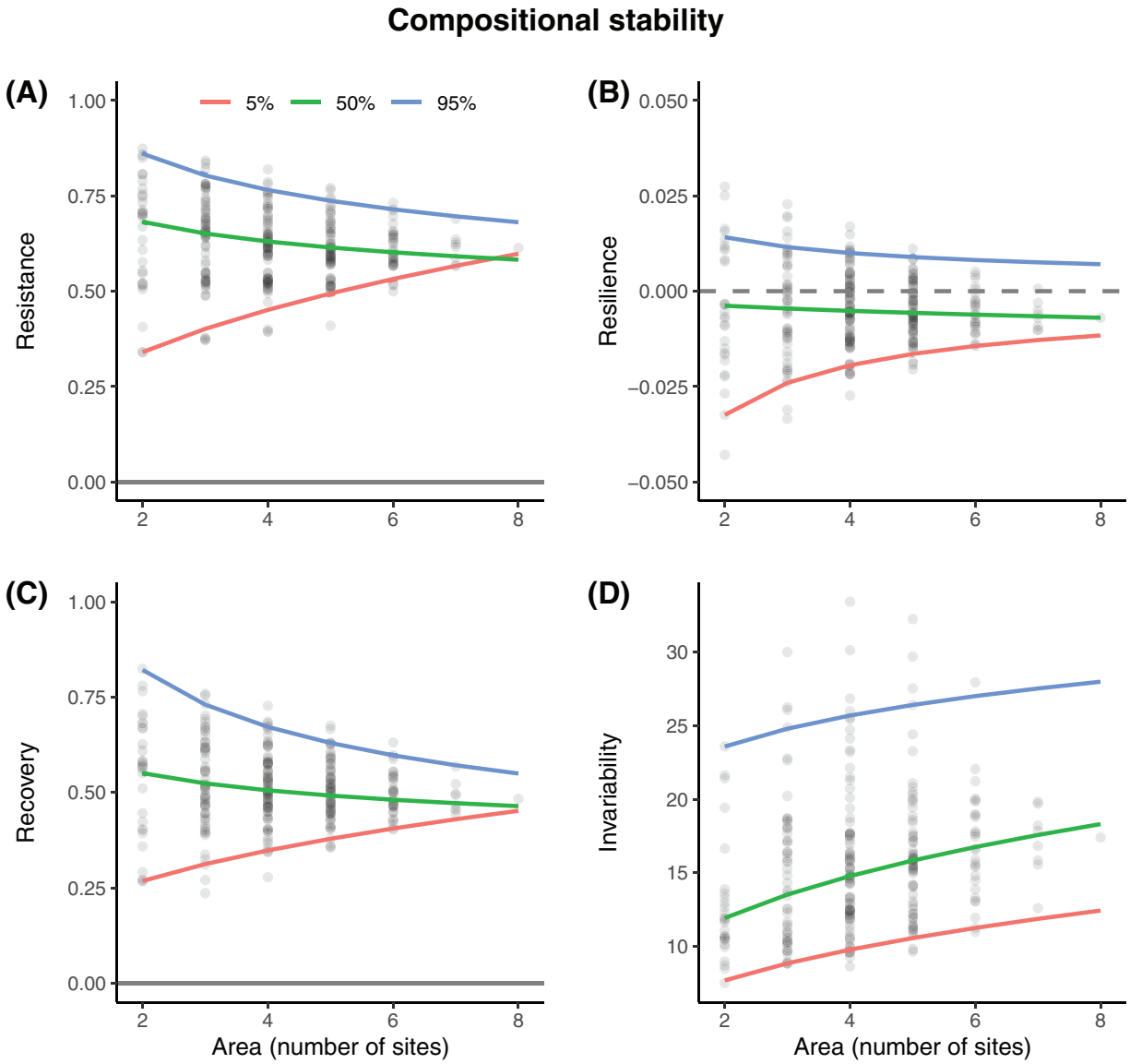

Figure 5. Compositional stability across areas (*A*) in marine macrobenthic intertidal communities in response to the experimental removal of the locally dominant species. The horizontal continuous grey line indicates maximal stability for resistance and recovery. The horizontal dashed grey line denotes minimal resilience. Blue, green, and red lines represent the predicted values of quantile nonlinear models for the 95%, 50% and5% quantiles, respectively.

continental-scale productivity (Wang et al. 2017). Future field manipulative research in the study region should extend the spatial range examined to detect in full the predicted triphasic invariability–area relationship. Nevertheless, our experimental manipulations replicated in several communities revealed novel empirical scale-dependent patterns for compositional invariability and other stability dimensions (Clark et al. 2021 for extrapolated scaling relationships).

The use of percentage cover as a proxy for species abundances and an aggregate community-level property allowed us to analyse the spatial scaling of stability in both composition and function, respectively. However, this metric can pose the drawback that the upper limit of the variance is constrained, which could generate spurious compensatory dynamics. To overcome this issue and allow the summed cover to exceed 100%, we considered organisms growing on both rock and other organisms, as done in previous manipulative studies conducted in rocky intertidal communities (Donohue et al. 2013, Mrowicki et al. 2016, White et al. 2020). Moreover, those studies demonstrate that percentage cover correlates well with biomass, an important functional proxy. This also allowed us to further incorporate the outcome of facilitative interactions between primary space-holders (e.g. mussels) and secondary space-holders (e.g. barnacles and macroalgae), and between canopy forming macroalgae and understorey species (e.g. turfs). Previous works based on biomass support our results based on cover (Hillebrand et al. 2018). In addition, percentage cover, biomass, and individual frequencies

have been shown to yield similar results in terms functional (total abundance) invariability and synchrony in species abundances (Valencia et al. 2020). Therefore, cover can be a useful proxy for both functional and compositional variables of sessile communities, where a complex interaction among competition for space, disturbance and propagule pressure takes place (Paine 1980).

Stability dimensionality and domains: future prospects for conservation and management

We observed similar responses of different dimensions of stability to increasing area across both, functional and compositional domains. However, the recovery of the larger areas was more complete for function than composition. Within larger areas, thus, some level of species compensation might have allowed different communities to perform similar functioning. Indeed, recent local-scale analyses of the stability in this region demonstrate weak function–composition correlations for resistance and invariability, and negative correlations for resilience and recovery (Valdivia et al. 2021a). Comparable results have been found by mesocosm experiments demonstrating weak or negative function–composition correlations across stability dimensions (Guelzow et al. 2017, Hillebrand et al. 2018). Our results suggest that a larger area should improve the resistance, recovery, and invariability of regions facing a severe chronic disturbance, such as the extinction of the locally dominant species and habitat loss (Chase et al. 2020).

Our findings can provide insights into ecosystem conservation with central implications for the design of future management strategies (Waltham et al. 2020). Ecosystem restoration, for instance, has usually targeted the assessment of few stability dimensions, which could well be uncorrelated (Donohue et al. 2016, Moreno-Mateos et al. 2020). Thus, ecosystem management should explicitly consider multiple stability dimensions, accounting for the functional and compositional responses of regions to natural and anthropogenic disturbances. This can aid management efforts to set the appropriate steps and timing for each adaptive and unassisted recovery phase of restoration (Moreno-Mateos et al. 2020). Moreover, our results provide experimental evidence supporting the relevance of enlarging protected areas, rather than targeting particular habitat patches, to allow regional ecosystems to resist and recover from large-scale disturbances (Economo 2011, Chase et al. 2020, Ospina-Alvarez et al. 2020).

Conclusion

Here, we have shown that the resistance, recovery, and invariability of a large rocky intertidal region characterised by competition for space, disturbance, and recolonisation increased across spatial scales. Using the number of sites as a proxy for area, we demonstrated that smaller areas further departed from the reference condition after the experimental extirpation of the locally space-dominant species – this response was expressed as both functional overcompensation and compositional perturbations. The effect of area on stability was associated with area-dependent changes in beta diversity and community-level spatial synchrony in function. Finally, recovery was more complete for function than composition in the case of the largest areas, implying that altered communities would achieve pre-disturbance functioning levels. This study provides experimental evidence for the positive effect of larger areas on the ability of ecosystems to resist and recover from chronic disturbances, with important consequences for ecosystem conservation and management.

Acknowledgements – We thank all the enthusiastic undergraduate interns (Escuela Biología Marina; UACh) and the Changolab (CEAZA-UAI) who provided invaluable help during the fieldwork. Melissa González, José Pantoja and Oscar Beytía were fundamental to complete the sampling schedule in the northern region. Miguel Lurgi and Matthew Bracken provided constructive criticism that greatly improved an early version of this manuscript.
Funding – This study was financially supported by the FONDECYT no. 1190529, FONDECYT no. 1141037, and FONDAP no. 15150003 (IDEAL) grants to NV. MAA was supported by FONDECYT no. 1160223 and PAI-CONICYT no. 79150002-2016. BRB acknowledges the support of FONDECYT no. 1181300 and the UPWELL and MUSEL Millennium Nucleus, both funded by Iniciativa Científica Milenio.
Conflicts of interest – The authors declare no conflicts of interest.
Permits – The study did not need permits, because all experiments were conducted on open-access coastal areas.

Author contributions

Nelson Valdivia: Conceptualization (lead); Data curation (lead); Formal analysis (lead); Funding acquisition (lead); Investigation (lead); Methodology (lead); Project administration (lead); Resources (lead); Software (lead); Supervision (lead); Validation (lead); Visualization (lead); Writing-original draft (lead); Writing – review and editing (lead). **Daniela N. Lopez**: Data curation (equal); Investigation (equal); Methodology (equal); Project administration (equal); Writing – review and editing (equal). **Eliseo Fica-Rojas**: Data curation (equal); Investigation (equal); Methodology (equal); Writing – review and editing (equal). **Alexis M. Catalán**: Data curation (equal); Investigation (equal); Methodology (equal); Writing – review and editing. **Moisés A. Aguilera**: Writing – review and editing (equal). **Marjorie Araya**: Investigation (supporting); Methodology (supporting); Writing – review and editing (supporting). **Claudia Betancourtt**: Investigation (supporting); Methodology (supporting); Writing – review and editing (supporting). **Katherine Burgos-Andrade**: Investigation (supporting); Methodology (supporting); Writing – review and editing (supporting). **Thais Carvajal-Baldeon**: Investigation (supporting); Methodology (supporting); Writing – review and editing (supporting). **Valentina Escares**: Investigation (supporting); Methodology (supporting); Writing – review and editing (supporting). **Simon Gartenstein**: Investigation (supporting); Methodology (supporting); Writing – review and

editing (supporting). **Mariana Grossmann**: Investigation (supporting); Methodology (supporting); Writing – review and editing (supporting). **Bárbara Gutiérrez**: Investigation (supporting); Methodology (supporting); Writing – review and editing (supporting). **Jonne Kotta**: Writing – review and editing (equal). **Diego F. Morales-Torres**: Investigation (supporting); Methodology (supporting); Writing – review and editing (supporting). **Bárbara Riedemann-Saldivia**: Investigation (supporting); Methodology (supporting); Writing – review and editing (supporting). **Sara M. Rodríguez**: Investigation (supporting); Methodology (supporting); Writing – review and editing (supporting). **Catalina Velasco-Charpentier**: Investigation (supporting); Methodology (supporting); Writing – review and editing (supporting). **Vicente I. Villalobos**: Investigation (supporting); Methodology (supporting); Visualization (supporting); Writing – review and editing (supporting). **Bernardo R. Broitman**: Conceptualization (equal); Funding acquisition (equal); Supervision (equal); Writing – review and editing (equal).

Data availability statement

Data available from the Dryad Digital Repository: <http://dx.doi.org/10.5061/dryad.stqjq2c3f> (Valdivia et al. 2021b).

References

Aguilera, M. A., et al. 2019. Chapter 29 – Chile: environmental status and future perspectives. – In: Sheppard, C. (ed.), World seas: an environmental evaluation, 2nd edn. Academic Press, pp. 673–702.

Barton, P. S., et al. 2013. The spatial scaling of beta diversity. – Global Ecol. Biogeogr. 22: 639–647.

Baselga, A., et al. 2018. betapart: partitioning beta diversity into turnover and nestedness components. – R package ver. 151, <https://CRAN.R-project.org/package=betapart>.

Beck, J. et al. 2013. Undersampling and the measurement of beta diversity. – Methods Ecol. Evol. 4: 370–382.

Bracken, M. E. S. et al. 2017. Spatial scale mediates the effects of biodiversity on marine primary producers. – Ecology 98: 1434–1443.

Broitman, B. R. et al. 2001. Geographic variation of southeastern Pacific intertidal communities. – Mar. Ecol. Prog. Ser. 224: 21–34.

Broitman, B. R. et al. 2011. Geographic variation in diversity of wave exposed rocky intertidal communities along central Chile. – Rev. Chil. Hist. Nat. 84: 143–154.

Bruno, J. F. et al. 2003. Inclusion of facilitation into ecological theory. – Trends Ecol. Evol. 18: 119–125.

Bulleri, F. et al. 2012. Temporal stability of European rocky shore assemblages: variation across a latitudinal gradient and the role of habitat-formers. – Oikos 121: 1801–1809.

Camus, P. A. 2001. Marine biogeography of continental Chile. – Rev. Chil. Hist. Nat. 74: 587–617.

Chase, J. M. et al. 2020. Ecosystem decay exacerbates biodiversity loss with habitat loss. – Nature 584: 238–243.

Chesson, P. 2000. Mechanisms of maintenance of species diversity. – Annu. Rev. Ecol. Syst. 31: 343–366.

Clark, A. T. et al. 2021. General statistical scaling laws for stability in ecological systems. – Ecol. Lett. doi: 10.1111/ele.13760.

Delsol, R. et al. 2018. The relationship between the spatial scaling of biodiversity and ecosystem stability. – Global Ecol. Biogeogr. 27: 439–449.

Donohue, I. et al. 2016. Navigating the complexity of ecological stability. – Ecol. Lett. 19: 1172–1185.

Donohue, I. et al. 2013. On the dimensionality of ecological stability. – Ecol. Lett. 16: 421–429.

Dunstan, P. K. and Johnson, C. R. 2006. Linking richness, community variability, and invasion resistance with patch size. – Ecology 87: 2842–2850.

Economo, E. P. 2011. Biodiversity conservation in metacommunity networks: linking pattern and persistence. – Am. Nat. 177: E167–E180.

Eriksson, B. K. et al. 2006. Biotic habitat complexity controls species diversity and nutrient effects on net biomass production. – Ecology 87: 246–254.

Fenberg, P. B. et al. 2015. Biogeographic structure of the northeastern Pacific rocky intertidal: the role of upwelling and dispersal to drive patterns. – Ecography 38: 83–95.

Ferrari, S. L. P. and Cribari-Neto, F. 2004. Beta regression for modelling rates and proportions. – J. Appl. Stat. 31: 799–815.

France, K. E. and Duffy, J. E. 2006. Diversity and dispersal interactively affect predictability of ecosystem function. – Nature 441: 1139–1143.

Fukami, T. et al. 2001. On similarity among local communities in biodiversity experiments. – Oikos 95: 340–348.

Garreaud, R. D. et al. 2011. VOCALS-CUpEx: the Chilean upwelling experiment. – Atmos. Chem. Phys. 11: 2015–2029.

Gonzalez, A. et al. 2020. Scaling-up biodiversity–ecosystem functioning research. – Ecol. Lett. 23: 757–776.

Grimm, V. and Wissel, C. 1997. Babel, or the ecological stability discussions: an inventory and analysis of terminology and a guide for avoiding confusion. – Oecologia 109: 323–334.

Gruen, B. et al. 2012. Extended beta regression in R: shaken, stirred, mixed, and partitioned. – J. Stat. Softw. 48: 1–25.

Guelzow, N. et al. 2017. Functional and structural stability are linked in phytoplankton metacommunities of different connectivity. – Ecography 40: 719–732.

Harrison, G. W. 1979. Stability under environmental stress: resistance, resilience, persistence, and variability. – Am. Nat. 113: 659–669.

Hillebrand, H. et al. 2018. Decomposing multiple dimensions of stability in global change experiments. – Ecol. Lett. 21: 21–30.

Holling, C. S. 1973. Resilience and stability of ecological systems. – Annu. Rev. Ecol. Syst. 4: 1–23.

Holling, C. S. 1996. Engineering resilience versus ecological resilience. – In: Schulze, P. (ed.), Engineering within ecological constraints. – National Academies Press, pp. 31–44.

Hormazabal, S. et al. 2004. Coastal transition zone off Chile. – J. Geophys. Res. C. 109: C01021.

Hyman, A. C. et al. 2019. Long-term persistence of structured habitats: seagrass meadows as enduring hotspots of biodiversity and faunal stability. – Proc. R. Soc. B 286: 20191861.

Isbell, F. et al. 2017. Linking the influence and dependence of people on biodiversity across scales. – Nature 546: 65–72.

Ives, A. R. and Carpenter, S. R. 2007. Stability and diversity of ecosystems. – Science 317: 58–62.

Jaccard, P. 1900. Contribution au problème de l'immigration postglaciaire de la flore alpine : étude comparative de la flore alpine

du massif de Wildhorn, du haut bassin du Trient et de la haute vallée de Bagnes. – Bull. Soc. Vaudoise Sci. Nat. 36: 87–130.
Jones, C. G. et al. 1994. Organisms as ecosystem engineers. – Oikos 69: 373–386.
Jørgensen, S. E. and Nielsen, S. N. 2013. The properties of the ecological hierarchy and their application as ecological indicators. – Ecol. Indic. 28: 48–53.
Jurgens, L. J. and Gaylord, B. 2018. Physical effects of habitat-forming species override latitudinal trends in temperature. – Ecol. Lett. 21: 190–196.
Kéfi, S. et al. 2019. Advancing our understanding of ecological stability. – Ecol. Lett. 22: 1349–1356.
Koenker, R. 2020. quantreg: quantile regression. – R package ver. 555.
Lande, R. et al. 1999. Spatial scale of population synchrony: environmental correlation versus dispersal and density regulation. – Am. Nat. 154: 271–281.
Lara, C. et al. 2019. Coastal biophysical processes and the biogeography of rocky intertidal species along the south-eastern Pacific. – J. Biogeogr. 46: 420–431.
Legendre, P. and Legendre, L. 1998. Numerical ecology. – Elsevier.
Loreau, M. et al. 2003. Biodiversity as spatial insurance in heterogeneous landscapes. – Proc. Natl Acad. Sci. USA 100: 12765–12770.
Menge, B. A. et al. 2015. Are meta-ecosystems organized hierarchically? A model and test in rocky intertidal habitats. – Ecol. Monogr. 85: 213–233.
Micheli, F. et al. 1999. The dual nature of community variability. – Oikos 85: 161–169.
Moreno-Mateos, D. et al. 2020. The long-term restoration of ecosystem complexity. – Nat. Ecol. Evol. 4: 676–685.
Morgan, S. G. et al. 2009. Nearshore larval retention in a region of strong upwelling and recruitment limitation. – Ecology 90: 3489–3502.
Mori, A. S. et al. 2018. β-diversity, community assembly, and ecosystem functioning. – Trends Ecol. Evol. 33: 549–564.
Mrowicki, R. J. et al. 2016. Temporal variability of a single population can determine the vulnerability of communities to perturbations. – J. Ecol. 104: 887–897.
Odum, E. P. 1950. Bird populations of the Highlands (North Carolina) plateau in relation to plant succession and avian invasion. – Ecology 31: 587–605.
Oksanen, J. et al. 2019. vegan: community ecology package. – R package ver. 25–6.
Ospina-Alvarez, A. et al. 2020. Integration of biophysical connectivity in the spatial optimization of coastal ecosystem services. – Sci. Total. Environ. 733: 139367.
Paine, R. T. 1980. Food webs: linkage, interaction strength and community infrastructure. – J. Anim. Ecol. 49: 667–685.
Peterson, G. et al. 1998. Ecological resilience, biodiversity, and scale. – Ecosystems 1: 6–18.
Pimm, S. L. 1984. The complexity and stability of ecosystems. – Nature 307: 321–326.
Pinochet, A. et al. 2019. Seasonal variability of upwelling off central-southern Chile. – Remote Sens. 11: 1737–1751.
Radchuk, V. et al. 2019. The dimensionality of stability depends on disturbance type. – Ecol. Lett. 22: 674–684.
Rius, M. et al. 2017. Ecological dominance along rocky shores, with a focus on intertidal ascidians. – Oceanogr. Mar. Biol. 55: 55–84.
Roughgarden, J. et al. 1988. Recruitment dynamics in complex life cycles. – Science 241: 1460–1466.
Scheffer, M. et al. 2009. Early-warning signals for critical transitions. – Nature 461: 53–59.
Tennekes, M. 2018. tmap: thematic maps in R. – J. Stat. Softw. 84: 1–36.
Thiel, M. et al. 2007. The Humboldt Current System of northern and central Chile. – Oceanogr Mar. Biol. 45: 195–344.
Thompson, P. L. et al. 2020. A process-based metacommunity framework linking local and regional scale community ecology. – Ecol. Lett. 23: 1314–1329.
Tilman, D. 1996. Biodiversity: population versus ecosystem stability. – Ecology 77: 350–363.
Tilman, D. 1999. The ecological consequences of changes in biodiversity: a search for general principles. – Ecology 80: 1455–1474.
Ugland, K. I. et al. 2003. The species-accumulation curve and estimation of species richness. – J. Anim. Ecol. 72: 888–897.
Valdivia, N. et al. 2013. Mesoscale variation of mechanisms contributing to stability in rocky shore communities. – PLoS One 8: e54159.
Valdivia, N. et al. 2015. Disentangling the effects of propagule supply and environmental filtering on the spatial structure of a rocky shore metacommunity. – Mar. Ecol. Prog. Ser. 538: 67–79.
Valdivia, N. et al. 2021a. High dimensionality of the stability of a marine benthic ecosystem. – Front. Mar. Sci. 7.
Valdivia, N. et al. 2021b. Data from: Stability of rocky intertidal communities in response to species removal varies across spatial scales. – Dryad, <http://dx.doi.org/10.5061/dryad.stqjq2c3f>.
Valencia, E. et al. 2020. Synchrony matters more than species richness in plant community stability at a global scale. – Proc. Natl Acad. Sci. USA 117: 24345–24351.
Vellend, M. 2016. The theory of ecological communities (MPB-57). – Princeton Univ. Press.
Waltham, N. J. et al. 2020. UN decade on ecosystem restoration 2021–2030 – what chance for success in restoring coastal ecosystems? – Front. Mar. Sci. 7: 569650.
Wang, S. et al. 2017. An invariability–area relationship sheds new light on the spatial scaling of ecological stability. – Nat. Commun. 8: 15211.
Wang, S. P. et al. 2019. Stability and synchrony across ecological hierarchies in heterogeneous metacommunities: linking theory to data. – Ecography 42: 1200–1211.
Wang, S. P. and Loreau, M. 2014. Ecosystem stability in space: alpha, beta and gamma variability. – Ecol. Lett. 17: 891–901.
White, L. et al. 2020. Individual species provide multifaceted contributions to the stability of ecosystems. – Nat. Ecol. Evol. 4: 1594–1601.
Whittaker, R. H. 1972. Evolution and measurement of species diversity. – Taxon 21: 213–251.
Wickham, H. et al. 2019. Welcome to the tidyverse. – J. Open Source Softw. 4: 1686.
Wilke, C. O. 2016. cowplot: streamlined plot theme and plot annotations for 'ggplot2'. – R package ver. 100, <https://CRAN.R-project.org/package=cowplot>.
Wilsey, B. J. et al. 2014. Invaded grassland communities have altered stability-maintenance mechanisms but equal stability compared to native communities. – Ecol. Lett. 17: 92–100.